SPACECRAFT FORMATION FLYING MANEUVERS USING LINEAR-QUADRATIC REGULATION WITH NO RADIAL AXIS INPUTS

Scott R. Starin (NASA/GSFC), R. K. Yedavalli (Ohio State University) and Andrew G. Sparks (AFRL/VACA)

Abstract

Regarding multiple spacecraft formation flying, the observation has been made that control thrust need only be applied coplanar to the local horizon to achieve complete controllability of a two-satellite (leader-follower) formation. A formulation of orbital dynamics using the state of one satellite relative to another is used. Without the need for thrust along the radial (zenith-nadir) axis of the relative reference frame, propulsion system simplifications and weight reduction may be accomplished. Several linear-quadratic regulators (LQR) are explored and compared based on performance measures likely to be important to many missions, but not directly optimized in the LQR designs. Maneuver simulations are performed using commercial ODE solvers to propagate the Keplerian dynamics of a controlled satellite relative to an uncontrolled leader. These short maneuver simulations demonstrate the capacity of the controller to perform changes from one formation geometry to another. This work focusses on formations in which the controlled satellite has a relative trajectory which projects onto the local horizon of the uncontrolled satellite as a circle. This formation has potential uses for distributed remote sensing systems.

Introduction

The desire to minimize the space mission costs and risks associated with dependence on single, large spacecraft has contributed to the development of spacecraft formation flying technology. A considerable body of research (*cf.* [1-10]) has been directed toward the automatic control of the most basic satellite formation—two satellites flying in similar, nearly circular orbits. This formation, is sometimes called a leader-follower pair, and its dynamics are often represented by a first-order, nonlinear system of ordinary differential equations (ODEs) by defining a rotating frame of reference fixed to the leader satellite.

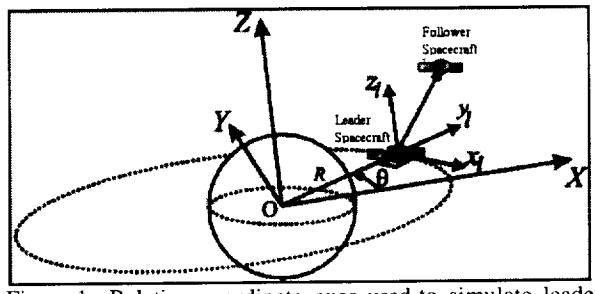

Figure 1: Relative coordinate axes used to simulate leader-follower formation dynamics. Figure courtesy of Mr. H. Wong.

Dynamical Representations

Let x represent the direction opposite the leader's orbital velocity (along-track); y, the direction from the Earth's center out to the leader's position (radial); and z, the direction parallel to the constant angular momentum of the leader's orbit (cross-track) (see Figure 1). Then the relative frame transformation of the Keplerian dynamics is given by

$$\ddot{x} = 2\omega\dot{y} + \omega^2 x[1 - g(x,y,z,r_{orbit})] + F_x \quad (1)$$

$$\ddot{y} = -2\omega\dot{x} + \omega^2 (y + r_{orbit})[1 - g(x,y,z,r_{orbit})] + F_y \quad (2)$$

$$\ddot{z} = -\omega^2 z\, g(x,y,z,r_{orbit}) + F_z \quad (3)$$

where r is the orbital radius of the leader, ω is the constant orbital rate, F_i $\{i=x,y,z\}$ denotes relative accelerations caused by control forces and external disturbances (including all non-Keplerian effects), and

$$g(x,y,z,r_{orbit}) \equiv \left[1 + \frac{2y}{r_{orbit}} + \frac{1}{r_{orbit}^2}(x^2 + y^2 + z^2)\right]^{-3/2} \quad (4)$$

These expressions are very similar to expressions already available in the literature, *cf.* Kapila.[10]

The nonlinear system of Eqs. 1–4 may be linearized using the leader's orbit as the origin. Such a linearization has the same effect as equating $g(x,y,z,r_{orbit})$ to unity; if the separation of the satellites is much less than their orbital radius, the term $g(x,y,z,r_{orbit}) \approx 1$, so that the nonlinear coupling terms become so weak that the system is essentially linear in character. The relative dynamics were first linearized by Clohessy and Wiltshire:[1]

$$\ddot{x} = 2\omega\dot{y} + F_x \quad (5)$$

$$\ddot{y} = -2\omega\dot{x} + 3\omega^2 x + F_y \quad (6)$$

$$\ddot{z} = -\omega^2 z + F_z, \quad (7)$$

It is often noted that this linearization allows the dynamics parallel to the orbital plane (x- and y-axes) to be decoupled from the dynamics perpendicular to that plane (z-axis). Since the so-called out-of-plane dynamical equations represent simple harmonic motion, and since the in-plane dynamics are bounded input-bounded output (BIBO) unstable, the out-of-plane dynamics are frequently set aside so that full attention may be given to the in-plane control problem. In this research the out-of-plane dynamics were included.

One useful state-space representation of Eqs. 5–7 is:

$$\dot{\underline{x}} = A\underline{x} + B\underline{u} \tag{8}$$

where the state and control vectors are

$$\underline{x} \equiv \begin{bmatrix} x & y & z & \dot{x} & \dot{y} & \dot{z} \end{bmatrix}^T \tag{9}$$

$$\underline{u} \equiv \begin{bmatrix} u_x & u_y & u_z \end{bmatrix}^T \tag{10}$$

and the state and control matrices are

$$A \equiv \begin{bmatrix} & 0_{3\times3} & & & I_{3\times3} & \\ 0 & 0 & 0 & 0 & 2\omega & 0 \\ 3\omega^2 & 0 & 0 & -2\omega & 0 & 0 \\ 0 & 0 & -\omega^2 & 0 & 0 & 0 \end{bmatrix}, \tag{11}$$

$$B \equiv \begin{bmatrix} 0_{3\times3} \\ I_{3\times3} \end{bmatrix}. \tag{12}$$

Strategy for Control of Leader-Follower Formations

The linearized form of the relative frame dynamics for the leader-follower formation has been known for some time. Linear-quadratic control of the leader-follower pair using control inputs along the along-track (x) and radial (y) axes has been partially explored.[7,11,12] The controllability of the in-plane dynamics has been observed and demonstrated by simulations.[7] Possible formation geometries have been explored, and sets of unforced formation trajectories, *i.e.*, formation trajectories which would be closed and stable without any control provided there are no deviations from purely Keplerian mechanics, have been detailed.[6,8]

In a previous paper[9], we noted the complete controllability of the in-plane dynamics state-space pair analogous to the full dynamics pair ($\mathbf{A},\mathbf{B}_x$), where $\mathbf{A}$ is given by Eq. 11, and

$$B_x \equiv \begin{bmatrix} & 0_{3\times2} & \\ 1 & & 0 \\ 0 & & 0 \\ 0 & & 1 \end{bmatrix}. \tag{13}$$

In the earlier work, maneuvers were simulated which occurred entirely within the x-y plane. However, this paper will include the out-of-plane dynamics to provide a better understanding of a maneuver that involves movement in all three dimensions.

Controllability inheres even though the definition of $\mathbf{B}_x$ given by Eq. 13 does not allow the radial input, u_y, to be included in the controller design. At least one other paper presents a successful design using only along-track inputs in the form of differential drag actuated by drag plates.[4] That design uses a nonlinear algorithm to effect correction maneuvers using only the input values $-a$, 0, and $+a$, where a is the magnitude of the relative acceleration created by placing the drag plates of the two spacecraft in different configurations. In contrast to this nonlinear design, the goal of our earlier paper was to validate the use of a linear control algorithm to command a strictly along-track control trajectory to the follower spacecraft based only on its position and velocity relative to the leader.

In this paper, we present simulations of linear-quadratic regulator (LQR) controllers without radial inputs performing certain maneuvers between initial and target trajectories. An error regulation scheme is employed where the origin of the state-space is not the target trajectory. In calculating controller gains based on regulation of the state (or the state error) of the follower satellite relative to the leader, we nondimensionalized the variables involved to reduce errors in calculation and to make the result more broadly applicable; Vassar and Sherwood have also used this nondimensionalization.[7] By also normalizing the orbital radius, the nondimensionalization had the effect of making the linear results applicable to all circular, Keplerian orbits. Note that after these conversions are performed, the orbital velocity, $v = \omega r_{orbit}$, is also unity.

Since LQR cannot be used directly to optimize such potentially important performance factors as fuel efficiency and time required for maneuver completion, the performance levels available to each type of controller—the type with and the type without radial inputs—were characterized over a selected range of gain matrices. The LQR cost function used to create most of the gain matrices and associated closed-loop systems examined is given by

$$J = \int_{t_0}^{t_f} \left(\underline{x}^T Q \underline{x} + \rho \underline{u}^T I \underline{u} \right) dt, \tag{14}$$

where $\mathbf{I}$ is the identity of appropriate dimension (2x2 without radial inputs or 3x3 with radial inputs). The scalar control weighting factor, ρ, was varied for both controller types to produce a suite of control gains for each type. A similar range of maneuvers was simulated for each suite of controllers. Then, the results of those simulations were interpreted according to several performance criteria that are not directly optimized by

the LQR design.

Simulations

Simulations of maneuvers from a constant x-axis offset (the "in-plane" formation of Sabol *et al.*[6]) to the origin were presented in earlier research.[9] In this paper we discuss simulations pertaining to a more complex formation in which the follower's elliptical trajectory in relative space projects a circle onto the local horizon of the leader. Sabol *et al.* refer to this as a "projected circular" formation.[6]

The projected circular formation is characterized by movement of the follower satellite about the leader along all three dimensions of the relative coordinate frame as defined above. In order to model this movement in maneuvers, we have included the cross-track (out-of-plane) dynamics in all simulations. To understand fully the effects of omitting radial inputs from leader-follower LQR controllers The simulation of these controllers was limited to purely Keplerian dynamics. Since long-term formationkeeping is only a non-trivial problem in the presence of non-Keplerian dynamics, these simulations were limited to the completion of finite maneuvers which placed a formation into a desired trajectory.

The relative state dynamics for a projected circular trajectory may be parameterized using only one independent variable. The independent variable may be time, or it may be the "phase" of the follower position on the projected circle, which is a linear function of time. The relative-frame parameterization of projected circular motion is given by:

$$x(t) = r_{circle}\cos\theta \tag{15}$$

$$y(t) = \frac{1}{2} r_{circle}\sin\theta \tag{16}$$

$$z(t) = \pm r_{circle}\sin\theta \tag{17}$$

where the phase angle is defined by

$$\theta \equiv \omega t + \theta_0 \tag{18}$$

and r_{circle} in this case corresponds to the radius of the projected circle and θ_0 is the phase angle at time t = 0. Note that θ is the angular displacement of the satellite's position relative to the leader, projected onto the x-z plane. This phase angle will become a useful descriptor of formation geometry in the exposition that follows this section.

As mentioned above, a suite of controller gains corresponding to each type of controller was obtained by varying the scalar control weighting factor, ρ, and minimizing the cost function in Eq. 14 for each value of ρ. For the linear simulations, ρ took on 19 values from 0.1 to 9.1 for each type of controller. To facilitate the evaluation of many similar controllers, the simulations were performed entirely within the relative coordinate frame. A proprietary fourth/fifth order Runge-Kutta ODE solver was used to propagate both the nonlinear equations (Eqs. 1–4) and the linearized equations (Eqs. 5–7) modeling the continuous-time relative dynamics of the leader-follower pair. For this part of the research (also presented in a Master's degree thesis[14]), the inertial frame was not used in any part of the simulations; this practice artificially guaranteed that the Keplerian dynamics would be unperturbed. Also, the formation sizes tested here all conform to the requirement that the separation be much less than the orbital radius of the formation. Therefore, these results apply only to the linear regime.

The typical simulation consisted of the regulation of an initial projected circular trajectory to the origin of the state space. By strict interpretation, this regulation would have the effect of bringing the follower satellite to exactly the same position as the leader satellite in the relative frame, thereby causing a collision. In fact, the maneuver also represents one method of moving from a larger projected circular trajectory to a smaller one (or from a smaller to a larger, within limits), wherein a specified moving point on the desired projected circle is the target of the follower. The method is, in essence, to postulate an artificial "leader" which follows the target trajectory, to transform the coordinates to relocate the state-space origin at the artificial leader's location, and then to use LQR to "collide" with the new origin. This simplification of the tracking problem is applicable since, as mentioned by Carpenter, the state error obeys the same dynamical equations as the state itself.[12] Said another way, the state-space representations given as Eqs. 8–12 and Eqs. 8–11,13 are applicable no matter what the choice of origin, so long as the constraint $x,y,z \ll r_{orbit}$ is obeyed. The appendix to this paper derives expressions which assist in the transformation of the problem of changing the size of a projected circular formation to the regulation problem simulated by the authors.

This maneuver was simulated for projected circular trajectories of several appropriate initial nondimensional radii, on the order of 10^{-5}–10^{-4}. By properly choosing the velocity, maneuver simulations were also initialized at various phase angles, θ_0, of a projected circular trajectory as defined in Eq. 18. Each maneuver was considered complete when the point-mass spacecraft had reached a predetermined completion threshold. This threshold was defined by a separation of 5% of the initial formation radius, r_0, and a relative velocity of 1% of ωr_0, the product of orbital rate and initial formation radius. The purpose of the threshold

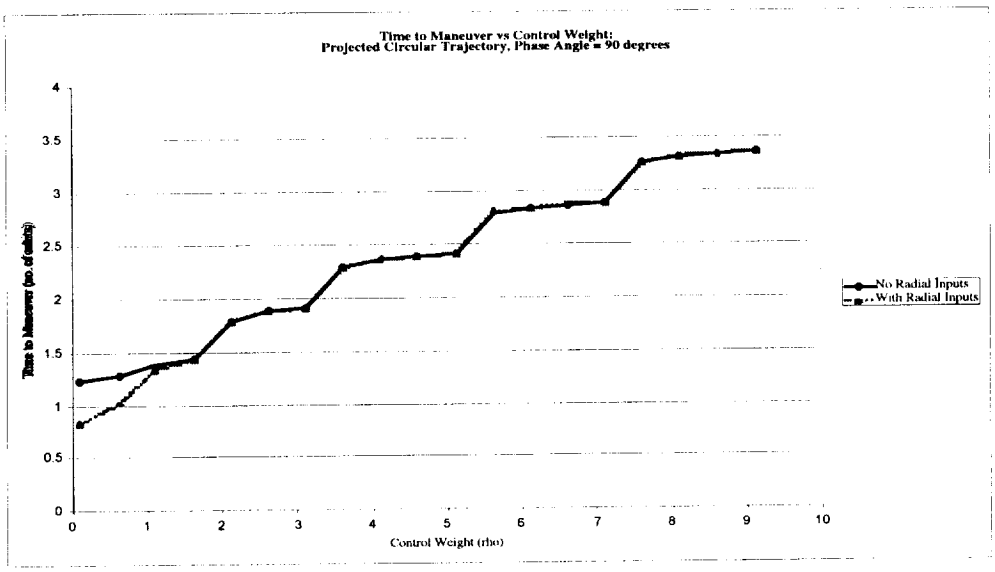

Figure 2: Time to maneuver, t_{man}, *vs.* control weight, ρ, for controllers with and without radial inputs.

definition is to enable comparison between various controllers, and not to provide an absolute standard of maneuvering speed; any reasonably defined settling time threshold could have been used.

As would be expected from a linear system, the state and control trajectories resulting from these different initial radii were geometrically similar. That is, if the state and control trajectories were normalized in their length by the initial formation radius, then the trajectories were identical for all initial radii simulated using the same initial phase angle. Since this similarity rule was confirmed for many combinations of radius and phase angle, it was concluded that the simulation of a single maneuver with a given initial phase angle, θ_0, sufficed to characterize the linear behavior for all maneuvers with the same θ_0. Because of the similarity, all results obtained have been condensed by presenting here only simulation results for a maneuver with an initial formation radius of 1.5×10^{-5} orbital radii; these results should be recognized as being applicable to a range from 10^{-6}–10^{-4} orbital radii. For an orbit with radius 7000 km, this initial formation radius corresponds to a separation of 105 meters. This range of formation sizes yields nearly identical results for analogous linear and nonlinear simulations without perturbations[9].

Results

This section presents the results of simulations of maneuvers beginning at various states, denoted by phase angles, on a given projected circular trajectory and ending at the origin of the state-space. These simulations consisted of numerical propagation of the Clohessy-Wiltshire equations, Eqs. 5–7. All closed-loop systems tested were asymptotically stable within the limits of the linearization, as would be expected from the controllability of the pair (A,B_x).

The state and control trajectories for the various simulation runs were used to determine several performance factors that were not directly optimized by the LQR design method. Performance factors for each of the 38 control gain sets tested (19 values of ρ used with and without radial inputs) were calculated for a range of initial phase angles, $0° \le \theta_0 \le 180°$. The performance factors discussed here are: t_{man}, the time required to reach the maneuver completion threshold described above; u_{max}, the maximum control acceleration commanded by the LQR law; and m_{fuel}, the total fuel consumed during the maneuver. The fuel consumed was calculated by summing the time integrals of the absolute values of the accelerations ordered along each axis: *i.e.*

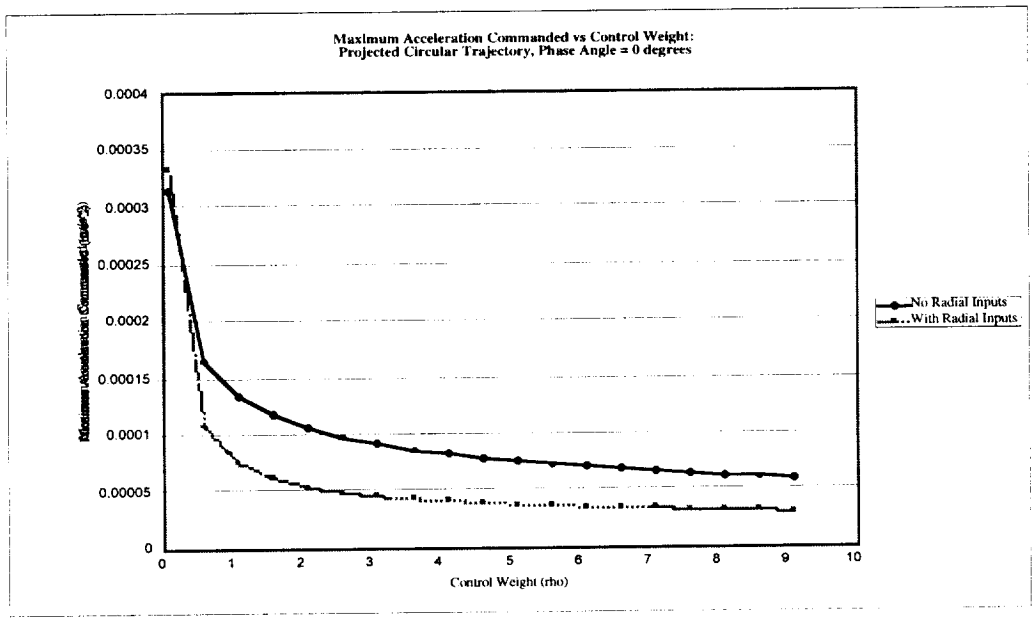

Figure 3: Maximum acceleration commanded, u_{max}, *vs.* control weight, ρ. Units are for a formation flying at an altitude of approx. 700 km (R_{orbit} = 7000 km). No pulse quantization was included in these simulations.

$$m_{fuel} = K \sum_{i} \int_{t_{initial}}^{t_{final}} |u_i| dt, \qquad i = x, y, z \qquad (19)$$

This fuel use calculation is consistent with a propulsion system that has pairs of thrusters aligned with each of the controlled axes; the constant K is proportional to the ratio of spacecraft mass to specific impulse. By contrast the integral of the control effort, $\int \underline{u}^T \underline{u}$ dt, which is included in the cost function defined in Eq. 14, would be consistent with a single thruster pair that is vectored by the controller.

The factor t_{man} depends very little on control weight, ρ, as illustrated in Figure 2. The figure shows results for an initial phase angle of $\theta_0 = 90°$, but since the effects of θ_0 on t_{man} are small overall, this figure is representative of all values of θ_0 tested. The stairstep shape of the plot is a result of time quantization in the simulation. Most notable in these results is that those results corresponding to the controllers without radial inputs follow exactly those corresponding to the use of radial inputs for all $\rho > 1$. Thus, there is no appreciable difference in the maneuvering speed of the two types of controllers at values of ρ which favor control effort optimization over state optimization (signified by $\rho >$ 1). However, if $\rho < 1$, indicating that adherence to the state trajectory is favored over optimization of control effort, the optimal trajectory in the absence of radial inputs is somewhat slower than that obtained from the inclusion of radial inputs.

The maximum acceleration, u_{max}, required for the optimal trajectory was more dependent upon the use of radial inputs. The absence of radial inputs resulted in a higher u_{max} for a given value of ρ and starting at θ_0 = 0° (Figure 3). So, for the controller without radial inputs to have the same value of u_{max} as with radial inputs, a higher value of ρ is required. The dependence of u_{max} upon phase angle is different for each type of controller, as can be seen in Figure 4, which plots the average value of u_{max} over all values of ρ tested for each combination of inputs and θ_0. For maneuvers with $\theta_0 \leq 120°$, the values of u_{max} commanded by controllers with radial inputs show little dependence upon θ_0, whereas the behavior of controllers without radial inputs shows a sinusoidal dependence over all values of θ_0 simulated.

Fuel consumption, represented by the performance factor m_{fuel}, showed a similar dependence on θ_0 to that of u_{max}; *i.e.*, having radial inputs available caused the fuel consumption of the optimal control trajectory to be less dependent on θ_0 (Figure 5). However, the comparison of values in the case of m_{fuel} is more favorable to the controller without radial inputs than was the comparison for u_{max}. The controller with radial inputs requires somewhat larger m_{fuel} near $\theta_0 = 90°$ than for other initial phase angles, and increasing θ_0 beyond 30° reduces the value of m_{fuel} consumed by the controllers without radial inputs.

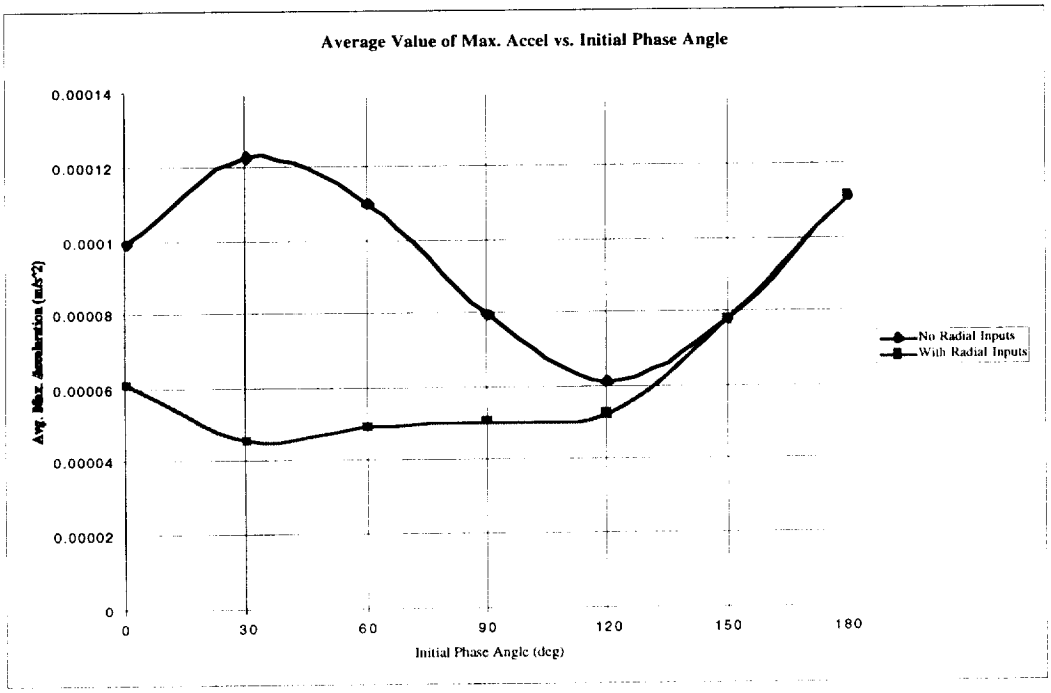

Figure 4: Average values of maximum acceleration commanded *vs.* initial phase angle for maneuver. Maximum accelerations were averaged over all tested values of control weight, ρ.

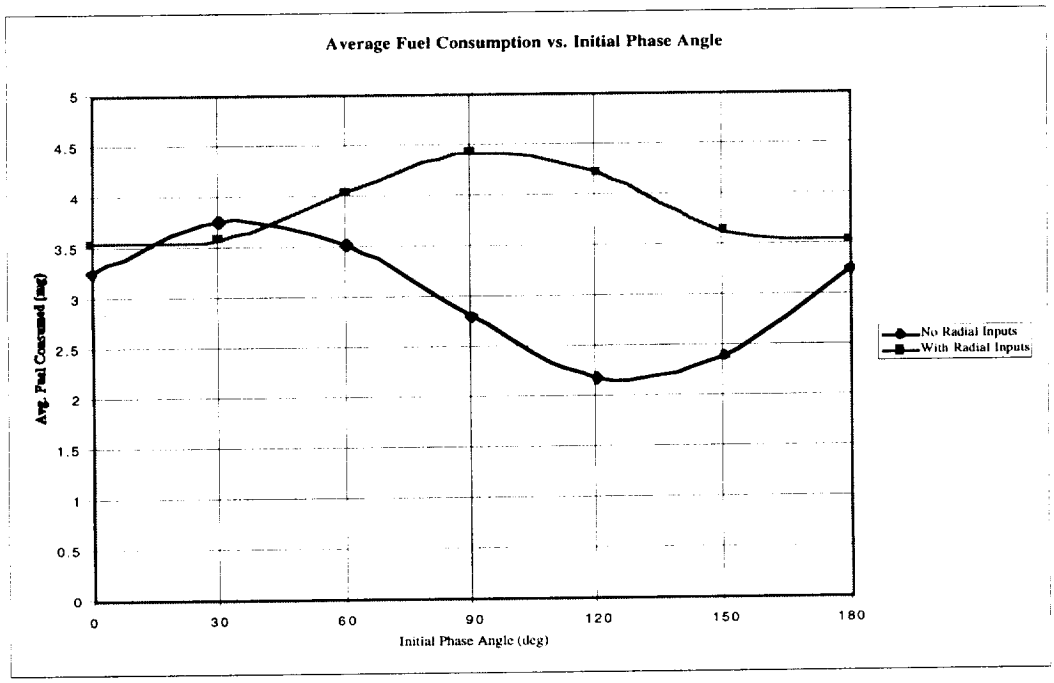

Figure 5: Average fuel consumption *vs.* initial phase angle, θ_0. Fuel consumption, m_{fuel}, averaged over range of control weights, ρ, for controllers with and without radial inputs. Appropriate units were calculated from the dimensionless results based on the following specifications: spacecraft mass = 100 kg; I_{sp} of hydrazine = 230 s; R_{orbit} = 7000 km.

Discussion

Figure 6 illustrates the optimal trajectory (projected onto the x-z plane) taken by a controller without radial inputs, with $\theta_0 = 90°$ and $\rho = 4$. Figure 7 shows the same maneuver with the same control weight $\rho = 4$, but performed through the additional use of radial inputs. At $\theta_0 = 90°$, the x-position variable is zero, the y- and z-position variables are at their maximum magnitudes, and the relative velocity is directed in the positive x-direction (*i.e.* the follower is slower than the leader in the inertial frame). Since the leader is in a circular trajectory, it can be said that the follower at $\theta_0 = 90°$ is at apoapse in its slightly elliptical orbit, since the altitude is at a maximum and the orbital velocity is at a minimum.

Between the two trajectories shown in Figures 6 and 7 there is no great variation. The chief difference between the two trajectories is something that proves true in most such comparisons made in this study: The use of radial inputs allows the follower to move more directly to the origin. In fact, the spacecraft without radial thrust can be seen to move initially further from the origin. This movement is the result of an initial strong thrust along the x-direction, which has the effect of changing the semi-major axis. The availability of radial thrust allows the follower sometimes to avoid this initial large thrust requirement; however, sometimes a greater fuel cost is incurred in using radial thrust for a maneuver of approximately the same t_{man} as can be obtained without radial thrust.

The improvements in fuel efficiency gained by removing radial inputs indicate an unexpected benefit to be gained by treating the radial inputs differently from the along-track and cross-track inputs. This observation is consistent with the results of the simulations of in-plane maneuvers in our earlier research.[9] The benefit may be interpreted to indicate the inclusion of astrodynamical principles in the LQR design. Often, the most fuel-efficient orbital maneuver thrusts are those which are most confined to the local horizontal plane— the plane spanned by the velocity vector of the leader (relative frame x-axis) and the vector perpendicular to the orbital plane (relative frame z-axis). This general principle may be applied to the majority of simple orbital maneuvers which follow Keplerian dynamics, including Hohmann transfers, low-thrust altitude changes, inclination changes, rotations of the eccentricity vector, *etc.* The orbital maneuvers which do not follow this principle, *e.g.* fast-transfers and rendezvous, are those maneuvers for which exact timing or swiftness of the maneuver is of greater importance than fuel efficiency.

By eliminating the y-axis inputs, which would be perpendicular to both of the efficient thrust directions, the controller without radial inputs decreases the probability of commanding inefficient thrust inputs. In the case of projected circular maneuvers presented here, the importance of phase angle discussed earlier provides more support for this astrodynamical interpretation, since the choice of θ_0 is effectively a choice of when to enact the strongest control thrust. If this strongest thrust is enacted at periapsis or apoapsis, the lack of radial thrust does not cause the controller to make greater demands on the propulsion system; u_{max} and m_{fuel} remain relatively low. But when the controller is required to begin at phase angles of $\theta_0 = 0°$ or $180°$, the lack of radial thrust becomes more troublesome.

Acknowledgments

This research was conducted through the support of the Air Force Research Laboratory and the NASA Goddard Space Flight Center. Mr. Starin's research effort was also funded by a graduate fellowship from The Ohio State University.

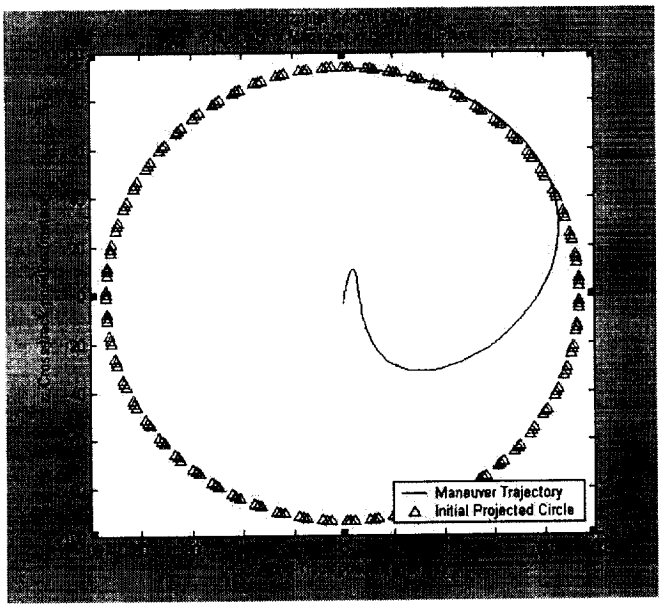

Figure 6: LQR maneuver trajectory from a projected circular trajectory to the origin using only horizontal thrust (*i.e.* no radial inputs). The maneuver started at θ_0= 90°, which is the point in the trajectory where the x-position is zero and the velocity is wholly in the +x direction. The movement along the y-direction (*i.e.* altitude change) is not pictured.

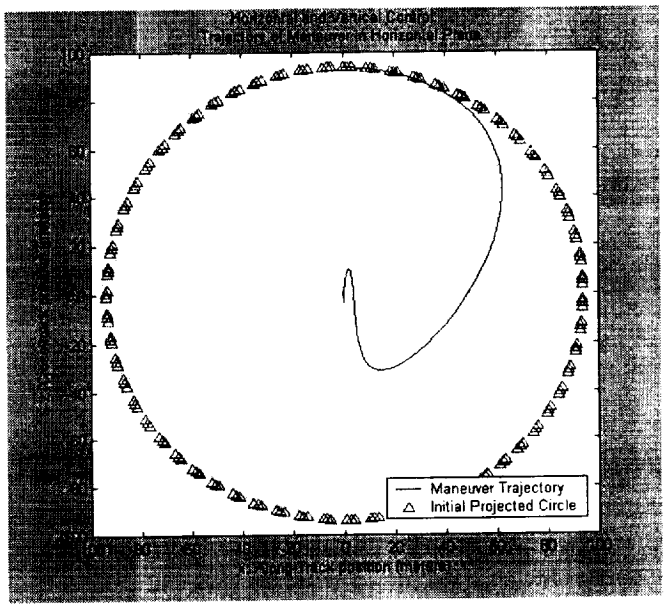

Figure 7: LQR maneuver trajectory from a projected circular trajectory to the origin using both horizontal and vertical, or radial, thrust. The maneuver started at θ_0= 90°. The movement along the y-direction (*i.e.* altitude change) is not pictured.

References

1. Clohessy, W. H. and R. S. Wiltshire, "Terminal Guidance System for Satellite Rendezvous", *J. Aerospace Sciences*, Vol. 27, No. 9, Sept 1960, pp. 653-658.

2. Inalhan, Gokhan, Franz D. Busse and Jonathan P. How, "Precise Formation Flying Control of Multiple Spacecraft Using Carrier-Phase Differential GPS", AAS 00-109, *AAS/AIAA Space Flight Mechanics Meeting*, Jan 2000.

3. Kumar, Renjith R. and Hans Seywald, "Fuel-Optimal Stationkeeping via Differential Inclusions", *J. Guid., Contr. & Dyn.*, Vol. 18, No. 5, Sept-Oct 1995, pp. 1156-1162.

4. Leonard, C. L., W. M. Hollister and E. V. Bergmann, "Orbital Formationkeeping with Differential Drag", *J. Guid., Nav. & Contr.*, Vol.12, No.1, 1989, pp.108-113.

5. Middour, Jay W., "Along Track Formationkeeping for Satellites with Low Eccentricity", *J. Astro. Sci.* Vol. 41, No. 1, Jan-Mar 1993, pp. 19-33.

6. Sabol, Chris, Richard Burns and Craig A. McLaughlin, "Satellite Formation Flying Design and Evolution", *AAS/AIAA Space Flight Mechanics Conference*, Feb 1999.

7. Vassar, Richard H. and Richard B. Sherwood, "Formationkeeping for a Pair of Satellites in a Circular Orbit", *J. Guid., Nav. & Contr.*, Vol. 8, No. 2, Mar-Apr 1985, pp. 235-242.

8. Yeh, Hsi-Han and Andrew Sparks, "Geometry and Control of Satellite Formations", *2000 American Control Conference*, Chicago, IL, Jun 2000.

9. Starin, Scott R., R.K. Yedavalli and Andrew G. Sparks, "Design of a LQR controller of reduced inputs for multiple spacecraft formation flying", *2001 American Control Conference*, Arlington, VA, Jun 2001.

10. Kapila, Vikram, "Spacecraft Formation Flying: A Survey", *Final Report for AFRL Summer Faculty Research Program*, Wright-Patterson AFB, OH, Sept 1998.

11. Ulybyshev, Yuri, "Long-Term Formation Keeping of Satellite Constellation Using Linear-Quadratic Controller", *J. Guid., Contr. & Dyn.*, Vol.21, No.1,1998, pp.109–115.

12. Carpenter, J. Russell, "Feasibility of decentralized linear-quadratic-gaussian control of autonomous distributed spacecraft", *NASA-GSFC Flight Mechanics Symposium*, NASA/CP–1999–209235, May 1999, pp. 345-357.

13. Schaub, H., S. R. Vadali, J. L. Junkins and K. T. Alfriend, "Spacecraft Formation Flying Control Using Mean Orbit Elements", AAS 99-310, *1999 Astrodynamics Conference*, AS, 1999.

14. Starin, Scott R., "Design of a linear control system of reduced inputs for multiple spacecraft formation flying", *Thesis for Master of Science*, The Ohio State University, Columbus, OH, August 2000.

APPENDIX

Theorem: Let two satellites be moving along coplanar, concentric projected circular trajectories: $x_1(t)$ with projected radius r_1, and $x_2(t)$ with projected radius r_2. Let these two trajectories share a common formation origin with a common coordinate system defined by the formation orbit (*i.e.* the orbit of the leader satellite). If one of these two satellites is defined as a new formation origin, then the trajectory, x*(t), of the other satellite about the first origin is also a projected circular trajectory inasmuch as the size of the formation fits within the constraints of linearization, $x,y,z << R_{orbit}$.

Proof: The parametric equations, as adapted from Yeh and Sparks[8], for the linearized trajectory of a satellite following a projected circular path relative to a leader satellite are provided as Eqs. 12-15 in the body of this paper. Note that $y(t) = \pm z(t)$ in these parametric equations. Furthermore, a positive sign on z(t) indicates counterclockwise movement as perceived from above the formation, and a negative sign indicates clockwise movement; the sign of z(t), once determined, will not change without considerable maneuvering. Therefore, the underlined $\underline{x}(t)$ will denote the projected position vector, $\underline{x}(t) = [x(t) \quad z(t)]^T$, since y(t) is implicit in this vector once the sign of z(t) is determined.

The linearized representation of the formation dynamics does not change with a change in formation origin for a formation in a nearly circular orbit. Consequently, the directions of the coordinate axes and the orbital angular momentum (vector $\underline{\omega}$) may all remain constant despite a change in origin. If $\underline{x}_1(t)$ denotes the projected trajectory of satellite #1, and $\underline{x}_2(t)$ the trajectory of satellite #2, then the trajectory of #2 with respect to #1 is obtained from differencing the two: $\underline{x}^*(t) = \underline{x}_2(t) - \underline{x}_1(t)$. By taking the dot product of each side of this equation with itself (*i.e.* the norm squared), and observing that the norms of $\underline{x}_1(t)$ and $\underline{x}_2(t)$ are the constant radii of their respective projected circles, the following result is obtained:

$$\left\|\underline{x}^*(t)\right\| = \left\|\underline{x}_2(t)\right\| + \left\|\underline{x}_1(t)\right\| - 2\left(\underline{x}_2(t)\cdot\underline{x}_1(t)\right) \qquad (A.1)$$

This relation is reminiscent of the law of cosines, since

$$\underline{x}_2(t)\cdot\underline{x}_1(t) = \left\|\underline{x}_2(t)\right\|\cdot\left\|\underline{x}_1(t)\right\|\cos(\varphi(t)) \qquad (A.2)$$

where $\varphi(t)$ is the angle between the vectors. For this particular case, the angle between the vectors may be obtained by differencing the two phase angles, $\varphi(t) = \theta_2(t) - \theta_1(t)$. Recalling the definition provided in Eq. 15, note that

$$\begin{aligned}\varphi(t) &= \theta_2(t) - \theta_1(t)\\ &= \left(\omega t + \theta_{02}\right) - \left(\omega t + \theta_{01}\right)\\ &= \theta_{02} - \theta_{01}\end{aligned} \qquad (A.3)$$

where θ_{02} and θ_{01} are the phase angles of the respective satellites at some initial time, t_0.
Because θ_{02} and θ_{01} are defined as constants, φ is also a constant in time.

Since the normed terms in Eq. A.1 are the constant formation radii and the left-hand side of Eq. A.2 is equal to a constant, then the norm of $\underline{x}^*(t)$ is constant. This means that the projection of this trajectory onto the local horizontal plane of satellite #1 (which is parallel to the local horizon of the original leader) is a circle. Furthermore, since the functions y(t) are all implicit in the representations of z(t), it follows that the trajectory $\underline{x}^*(t)$ is a projected circular trajectory. *Q.E.D.*

A bit more algebra provides expressions for the new projected circular trajectory in terms of the two old trajectories. Through use of the law of cosines, the radius of the new projected circle is given by

$$r^* = \sqrt{r_1^2 + r_2^2 - 2r_1r_2\cos\left(\theta_2 - \theta_1\right)} \qquad (A.4)$$

With some geometry combined with the law of sines, the phase angle, θ^*, of satellite #2 in its new projected circle may be derived as

$$\theta^*(t) = \theta_1(t) - \sin^{-1}\left(\frac{r_2}{r_1}\sin\theta_2(t)\right) \qquad (A.5)$$

The variables r*and θ^* may be transformed to x*, y*, and z* via the Eqs. 15-18 presented in the text. Then, the state vector used to calculate thrusts need only be redefined by subtracting the current desired state vector, *i.e.* $\underline{x}_{desired} \equiv \left[x^* \quad y^* \quad z^* \quad \dot{x}^* \quad \dot{y}^* \quad \dot{z}^*\right]^T$, from the current actual state. Thus the problem of changing the radius of a given projected circular trajectory to any other radius (within the limits of the linearization: $r_{1,2} << R_{orbit}$) may be reduced to a regulation problem which uses the same state-space representation, (**A**,**B**), as is used to regulate a projected circular trajectory to the origin.